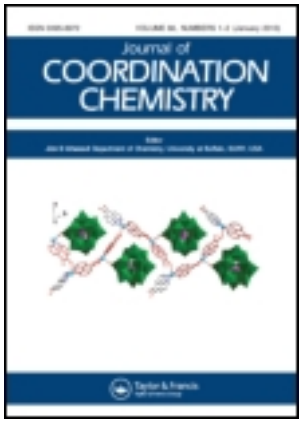

Journal of Coordination Chemistry
Publication details, including instructions for authors and subscription information:
http://www.tandfonline.com/loi/gcoo20

Copper(II) complexes of N,N′-dimethylethane-1,2-diamine with fluoride and tetrafluoroborate: syntheses, structures, and magnetic properties

Jaroslava Haníková [a], Juraj Kuchár [a], Erik Čižmár [b], Alexander Feher [b] & Juraj Černák [a]

[a] Department of Inorganic Chemistry, Institute of Chemistry, Faculty of Science, P. J. Šafárik University in Košice, Košice, Slovakia

[b] Department of Physics of Condensed Matters, Institute of Physics, Faculty of Science, P. J. Šafárik University in Košice, Košice, Slovakia

Accepted author version posted online: 07 Dec 2012.Published online: 22 Jan 2013.

To cite this article: Jaroslava Haníková, Juraj Kuchár, Erik Čižmár, Alexander Feher & Juraj Černák (2013) Copper(II) complexes of N,N′-dimethylethane-1,2-diamine with fluoride and tetrafluoroborate: syntheses, structures, and magnetic properties, Journal of Coordination Chemistry, 66:2, 316-328, DOI: 10.1080/00958972.2012.756978

To link to this article: http://dx.doi.org/10.1080/00958972.2012.756978

Journal of Coordination Chemistry
Vol. 66, No. 2, 20 January 2013, 316–328

Copper(II) complexes of *N*,*N*′-dimethylethane-1,2-diamine with fluoride and tetrafluoroborate: syntheses, structures, and magnetic properties

JAROSLAVA HANÍKOVÁ†, JURAJ KUCHÁR†, ERIK ČIŽMÁR‡, ALEXANDER FEHER‡ and JURAJ ČERNÁK*†

†Department of Inorganic Chemistry, Institute of Chemistry, Faculty of Science, P. J. Šafárik University in Košice, Košice, Slovakia; ‡Department of Physics of Condensed Matters, Institute of Physics, Faculty of Science, P. J. Šafárik University in Košice, Košice, Slovakia

(*Received 16 July 2012; in final form 11 October 2012*)

$[Cu(bmen)_2(H_2O)_2]F_2{\cdot}4H_2O$ (**1**) (*bmen* = *N*,*N*′-dimethylethane-1,2-diamine) and $[Cu(bmen)_2(BF_4)_2]$ (**2**) exhibit ionic and molecular crystal structures, respectively. In both **1** and **2,** Cu(II) exhibits tetragonally elongated six coordination in the 4 + 2 form with two chelate *bmen* in the equatorial plane; axial positions are occupied by weakly bound water in **1** while in **2** in these positions are fluorine from disordered BF_4^-. Packing in **1** and **2** are governed by hydrogen bonds (HBs). Magnetic studies from 1.8 to 300 K reveal that **1** and **2** follow the Curie–Weiss law with parameters $\theta = -0.88$ K and $g = 2.04$ for **1** and $\theta = -0.58$ K and $g = 2.13$ for **2**, suggesting the presence of weak antiferromagnetic interactions.

Keywords: Copper(II); Crystal structure; Hydrogen bond; Magnetic studies; Fluorine

1. Introduction

Hydrogen bonding mediated magnetism is well documented [1–3] and the exchange parameter *J* can reach as high value as 38.3 K [4]. Recent theoretical studies have demonstrated that hydrogen bonds (HBs) in mediating magnetic exchange interactions play only structural roles [5]. $[Cu(L{-}L)_2M(CN)_4]$ (*L*−*L* = *en* and its *N*-methylated derivatives and *M* = Ni, Pd, Pt) form 2,2-TT chain-like structures (for the nomenclature see [6b]) $[-(L{-}L)_2Cu{-}NC{-}M(CN)_2{-}CN{-}]_n$; HBs in these compounds play an important role in mediating magnetic exchange interactions [7–9]. As a continuation of these studies, we have prepared and characterized several complexes in which the tetracyanidometallate anions were replaced by fluorine-based anions [6a, 10]. For *L*−*L*-type blocking ligands, the use of fluorine-based anions led to the formation of a chain-like structure only for $[Cu(en)_2SiF_6]$ [10], otherwise different types of crystal structures were formed, e.g. ionic structure of $[Cu(deen)_2(BF_4)_2]$ (*deen* = *N*,*N*-diethylethylene-1,2-diamine) [11] or molecular structure of $[Cu(dien)(3Mpy)(BF_4)_2]$ (*dien* = N,N′,N″-diethylene-1,2-diamine;

*Corresponding author. Email: juraj.cernak@upjs.sk

Journal of Coordination Chemistry
ISSN 0095-8972 print/ISSN 1029-0389 online © 2012 Taylor & Francis
http://dx.doi.org/10.1080/00958972.2012.756978

3*Mpy* = 3-methyl-pyridine) [12]. Common feature of the prepared complexes is that Cu(II) are linked by HBs which involve the amine groups coordinated to Cu(II). Inspired by [Cu(*en*)$_2$(H$_2$O)$_2$]F$_2$·4H$_2$O [13] and [Cu(*en*)$_2$(BF$_4$)$_2$] [14], we have prepared analogous complexes in which *en* are replaced by symmetrically methylated *bmen* (*bmen* = *N,N′*-dimethylethane-1,2-diamine). Here, we report our results on syntheses, characterizations, crystal structures, spectroscopic and magnetic properties of [Cu(*bmen*)$_2$(H$_2$O)$_2$]F$_2$·4H$_2$O (**1**) and [Cu(*bmen*)$_2$(BF$_4$)$_2$)] (**2**).

2. Experimental

2.1. *Materials*

Copper(II) tetrafluoroborate hydrate Cu(BF$_4$)$_2$·*x*H$_2$O (98%, *x* = 6, 19–22% Cu, Aldrich), copper(II) fluoride hydrate CuF$_2$·*x*H$_2$O (*x* = 2, 98%, Aldrich), *bmen*, C$_4$H$_{12}$N$_2$ (98%, Aldrich) and methanol (analytical grade) were used as received.

2.2. *Syntheses of 1 and 2*

2.2.1. Synthesis of diaqua-bis(N,N′-dimethylethane-1,2-diamine)-copper(II) difluorido tetrahydrate, [Cu(*bmen*)$_2$(H$_2$O)$_2$]F$_2$·4H$_2$O (1). To 50 cm^3 of methanol, 0.54 cm^3 of *bmen* (5 mmol) and 0.5 g of CuF$_2$·2H$_2$O (5 mmol) were added and the reaction mixture was refluxed until complete dissolution of CuF$_2$·2H$_2$O (3 h). The resulting blue solution was filtered and left aside for crystallization. Within one month, blue–violet needles separated were filtered, washed quickly with small portion of water, and dried in air. Yield: 0.50 g (36%). Anal. Calc. for C$_8$H$_{36}$Cu$_1$F$_2$N$_4$O$_6$ (Mr = 385.94) (%): C, 24.90; H, 9.40; N, 14.52. Found: C, 25.32; 9.09; N, 13.99. IR (cm^{-1}; s = strong, m = medium, w = weak, v = very, sh = shoulder): 3424vs, 3226s, 3194sh, 3005m, 2966m, 2933m, 2810w, 1645s, 1525w, 1454s, 1367w, 1275m, 1157m, 1088m, 1058m, 1017s, 977s, 962m.

2.2.2. Synthesis of bis(N,N′-dimethylethane-1,2-diamine)-bis(tetrafluoroborate)-copper (II), [Cu(*bmen*)$_2$(BF$_4$)$_2$)] (2). Dropwise addition of *bmen* (0.22 cm^3, 2 mmol) to blue solution of Cu(BF$_4$)$_2$·*x*H$_2$O (*x* = 6, 0.2372 g, 1 mmol) in 10 cm^3 of water : propanol mixture (1 : 1 in vol.) yielded violet solution, which was filtered. After one month of crystallization, blue needles appeared which were separated by filtration and dried in air. Yield: 0.05 g (12%). Anal. Calc. for C$_8$H$_{24}$B$_2$Cu$_1$F$_8$N$_4$ (Mr = 413.47) (%): C, 23.24; H, 5.85; N, 13.97. Found: C, 23.17; H, 6.17; N, 13.29. Anal. Calc. for C$_8$H$_{24}$B$_2$Cu$_1$F$_8$N$_4$ (Mr = 413.46) (%): C, 23.24; H, 5.85; N, 13.55. Found: C, 23.17; H, 6.17; N, 13.29. IR (cm^{-1}; s = strong, m = medium, w = weak, vs = very strong, sh = shoulder): 3219s, 3186s, 2998w, 2964m, 2929s, 2810w, 1446s, 1119m, 1082vs, 1033m, 972vs, 857s, 772w, 530m.

2.3. *Physical measurements*

Elemental analyses (C, H, N) were performed on a CHNOS Elemental Analyzer vario MICRO. Infrared spectra were recorded on a FT-IR Avatar 330 Thermo-Nicolet instrument using KBr pellets (1 : 100) from 4000 to 400 cm^{-1}.

2.4. *Magnetic measurements*

Electron–paramagnetic resonance (EPR) data were collected in an X–band Bruker ELEXSYS E500 spectrometer from 1.8 to 300 K. The magnetic susceptibility (determined using the relation $\chi = M/H$) was taken at 0.01 and 0.1 T using a Quantum Design SQUID magnetometer (MPMS-XL5) from 1.8 to 300 K. The background contribution from the gelatine capsule to the magnetic moment of the sample has been subtracted. The obtained data were corrected for diamagnetic contribution using Pascal's constants and to temperature-independent paramagnetic contribution 60×10^{-6} emu/mol typical for Cu(II) [15]. The EPR and magnetic measurements have been carried out on polycrystalline samples.

2.5. *X-ray crystallography*

X-ray experiments were carried out on a four-circle κ axis Xcalibur2 diffractometer equipped with a CCD detector Sapphire2 (Oxford Diffraction). The CrysAlis software package [16] was used for data collection and reduction. Structures **1** and **2** were solved by direct methods and further refined using SHELXS-97 [17] and SHELXL-97 [17], incorporated in the WinGX program package [18]. During refinement of **2,** it became clear that BF_4^- was disordered. This disorder was modeled assuming that the anion occupies two disordered positions with a common boron; the refined s.o.f.'s were 0.685(13) : 0.315 (13). In order to keep the geometric parameters of these anions chemically reasonable, the B–F and F···F distances were constrained. Hydrogens in *bmen* in **1** and **2** were placed in calculated positions and allowed to ride on the parent with isotropic thermal parameters tied with the parent atoms (U(H) = 1.2U(CH2), U(H) = 1.5U(CH3), U(H) = 1.2U(N)). Water hydrogens in **1** were located with the program CALC–OH [19] and their isotropic thermal parameters were tied with the parent oxygens (U(H) = 1.5U(O)). Figures were drawn using Diamond software [20]. Crystal data and final parameters of the structure refinements for **1** and **2** are summarized in table 1, while selected geometric parameters are given in table 2. Possible HBs are gathered in tables 3 and 4.

3. Results and discussion

3.1. *Synthesis and identification*

From the alcohol/aqueous–alcohol systems Cu^{2+}–*bmen*–F^-/BF_4^-, $[Cu(bmen)_2(H_2O)_2]F_2{\cdot}4H_2O$ (**1**) and $[Cu(bmen)_2(BF_4)_2]$ (**2**) were isolated and characterized. Similar mild conditions were used for preparation of analogous compounds with *en* ligands $[Cu(en)_2(H_2O)_2]F_2{\cdot}4H_2O$ [13] and $[Cu(en)_2(BF_4)_2]$ [14] as well as for $[Cu(men)_2(BF_4)_2]$ [6a]. Analogous complex $[Cu(deen)_2(BF_4)_2]$ exhibits thermochromic behavior with transition temperature of 24 °C [11]. This possibility was checked for **2,** but we have not observed any color change from 4 to 150 °C.

3.2. *Spectroscopic characterization*

The presence of *bmen* in **1** and **2** is indicated by several absorptions. Those arising from N–H stretch were observed at 3226–3194 cm^{-1} and 3219–3186 cm^{-1} in **1** and **2**,

Table 1. Crystal data and structure refinement for **1** and **2**.

	1	**2**
Empirical formula	$CuC_8H_{36}N_4F_2O_6$	$CuC_8H_{24}N_4F_8B_2$
Formula weight	385.94	413.47
Temperature	290(2) K	173(2) K
Wavelength	0.71073 Å	0.71073 Å
Crystal system	Triclinic	Monoclinic
Space group	*P-1*	*C 2*
Unit cell dimensions	$a = 6.5995(5)$ Å	$a = 13.2501(4)$ Å
	$b = 8.2790(5)$ Å	$b = 8.8022(2)$ Å
	$c = 8.9517(7)$ Å	$c = 8.1356(3)$ Å
	$\alpha = 70.729(6)°$	$\alpha = 90°$
	$\beta = 73.559(6)°$	$\beta = 106.081(3)°$
	$\gamma = 78.572(5)°$	$\gamma = 90°$
Volume	439.84(5) Å^3	911.73(5) Å^3
Z	1	2
Density (calculated)	1.457 g.cm^{-3}	1.506 g.cm^{-3}
Absorption coefficient	1.289 mm^{-1}	1.270 mm^{-1}
Crystal dimensions	0.62 × 0.14 × 0.06 mm^3	0.45 × 0.27 × 0.26 mm^3
Theta range for data collection	3.04°–25.00°	3.20°–26.50°
Index ranges	$-7 \le h \le 7$,	$-16 \le h \le 16$,
	$-9 \le k \le 9$,	$-11 \le k \le 11$,
	$-10 \le l \le 10$	$-10 \le l \le 10$
Reflections coll./indep.	3616/1550 [R(int) = 0.0213]	9569/1885 [R(int) = 0.0210]
Absorption correction	Full-matrix least-squares on F^2	Full-matrix least-squares on F^2
Data/restraints/parameters	1550/9/117	1885/21/147
Goodness-of-fit on F^2	1.005	1.087
Final R indices [$I > 2\sigma(I)$]	$R1 = 0.0233$, w$R2 = 0.0493$	$R1 = 0.0514$, w$R2 = 0.1357$
R indices (all data)	$R1 = 0.0278$, w$R2 = 0.0502$	$R1 = 0.0520$, w$R2 = 0.1364$
Largest diff. peak and hole	0.218(4) and −0.158(4) e.Å^{-3}	0.688(9) and −0.285(9) e.Å^{-3}

Table 2. Selected geometric parameters [Å, °] for **1** and **2**.

1		**2**	
Cu1–N1	2.0280(14)	Cu1–N1	2.051(7)
Cu1–N2	2.0504(13)	Cu1–N2	2.018(7)
Cu1–O1	2.6703(14)	Cu1–F3	2.426(3)
N1–Cu1–N2	85.05(5)	Cu1–F7	2.629(8)
		N2–Cu1–N2	85.30(17)

respectively. The corresponding absorption bands in $[Cu(en)_2(H_2O)_2]F_2{\cdot}4H_2O$ were positioned at 3220–3130 cm^{-1} [13].

In the IR spectrum of **1,** the presence of water as ligands and molecules of crystallization shows by absorption bands at 3424 and 1645 cm^{-1}, ascribed to ν(OH) and $\delta(H_2O)$, respectively. The same absorption bands in $[Cu(en)_2(H_2O)_2]F_2{\cdot}4H_2O$ were at 3360 and 1640 cm^{-1} [13].

In the IR spectrum of **2,** strong absorptions at 1119, 1060, and 1033 cm^{-1} were observed, ascribed to $\nu(BF_4^-)$ vibrations [21]. In the spectrum of the analogous $[Cu(en)_2(BF_4)_2]$, the corresponding bands were at 1110, 1070, and 1037 cm^{-1} [22]. The presence of additional weaker absorptions of $\delta(BF_4^-)$ for **2** were observed at 772 and 530 cm^{-1}; for $[Cu(en)_2(BF_4)_2]$, corresponding bands at 770 and 521 cm^{-1} were reported [22].

Table 3. Possible HBs [Å, °] for **1**.

D–H···A	d(D–H)	d(H···A)	d(D···A)	<(DHA)
O1–H1O1···F1^{ii}	0.85	1.82	2.654(17)	169
O1–H2O1···O2^{iii}	0.85	1.99	2.838(19)	172
N1–H1···O1^{iv}	0.91	2.41	3.205(2)	146
N2–H2···F1^{v}	0.91	2.07	2.964(3)	169
O2–H1O2···F1^{iv}	0.85	1.84	2.691(18)	176
O2–H2O2···O3	0.85	1.97	2.809(19)	171
O3–H2O3···F1	0.85	1.98	2.826(17)	172
O3–H1O3···F1^{vi}	0.85	1.83	2.677(17)	177

Symmetry transformations used to generate equivalent atoms: (ii) 2−x, 1−y, −z; (iii) 1+x, y, z; (iv) −1+x, y, z; (v) x, −1+y, z; (vi) 1−x, 1−y, 1−z

Table 4. Possible HBs [Å, °] for **2**.

D–H···A	d(D–H)	d(H···A)	d(D···A)	<(DHA)
N1–H1···F5^{ii}	0.91	1.92	2.739(14)	149
N1–H1···F2^{ii}	0.91	2.36	2.958(11)	123
N2–H2···F8^{iii}	0.91	2.22	3.100(11)	162
N2–H2···F4^{iii}	0.91	2.50	3.139(11)	128

Symmetry transformations used to generate equivalent atoms: (i) −x, y, −z; (ii) 1/2+x, −1/2+y, z; (iii) 1/2+x, 1/2+y, z.

3.3. *Crystal structures*

3.3.1. [Cu(*bmen*)$_2$(H$_2$O)$_2$]F$_2$·4H$_2$O (1). The ionic crystal structure of **1** is analogous to the previously described crystal structure of [Cu(*en*)$_2$(H$_2$O)$_2$]F$_2$·4H$_2$O [13], composed of centrosymmetric *trans*-[Cu(*bmen*)$_2$(H$_2$O)$_2$]$^{2+}$, fluoride, and waters of crystallization (figure 1). Cu(II) is in the usual 4 + 2 distorted octahedral coordination. The observed geometric parameters in **1** within the complex cation are similar to those observed in the analogous *en* complex (table 2). The mean value for the Cu–N bond (2.039(11) Å) in **1** is somewhat longer than the corresponding one (2.021(3) Å) in [Cu(*en*)$_2$(H$_2$O)$_2$]$^{2+}$ [13]; similarly, somewhat longer (2.046(6) Å) Cu–N bond was also observed in [Cu(*bmen*)$_2$(H$_2$O)$_2$](*sac*)$_2$ (*sac* = *o*-sulfobenzimidate) [23]. The observed difference can be explained by the presence of large methyl substituent on the *N*-donor. In **1,** the aqua ligands in axial positions are at somewhat longer distances of 2.6703(14) Å (2*x*) as in the analogous *en* complex (2.571(6) Å) [13] or even in already-mentioned [Cu(*bmen*)$_2$(H$_2$O)$_2$](*sac*)$_2$ (2.5221(17) Å (2*x*)) [23]. It is suggested that the observed elongation of the already weak Cu–O (semi) bonds in **1** can be the consequence of the requirement to optimize the formed system of hydrogen bonding; the shortest O···F distance is 2.654(17) Å for O1 and F1^{ii} atoms (ii: $2-x, 1-y, -z$).

A remarkable feature of the crystal structure of **1** is its 3-D supramolecular hydrogen bonding system in which all hydrogens bonded to N and O as well as all fluorides are involved (table 3, figures 2(a)–(c)). The tilted CuN$_4$O$_2$, tetragonally elongated octahedra are arranged in line along the *a* axis (the angle between O–Cu–O and *a* axis is 38.80(3)°); the octahedra in this direction are linked by pairs of N1–H1···O1 HBs (O1 is from the neighboring octahedron, see table 3) leading to formation of $R_2^2(8)$ rings (for the nomen-

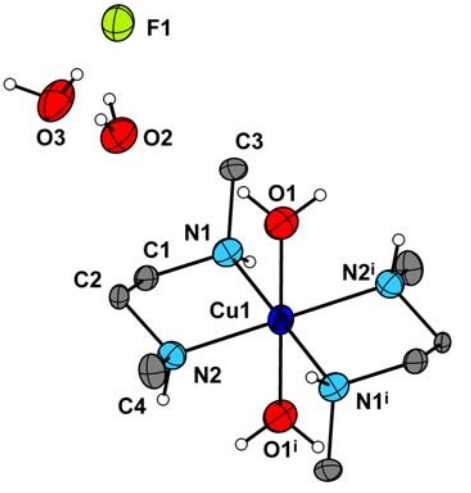

Figure 1. The ionic structure of **1**. Thermal ellipsoids were drawn at 50% probability level. Hydrogens from methyl and methylene from *bmen* are omitted for clarity. Symmetry code: i: $2-x, -y, -z$.

clature see [24, 25]). The (N2)H2 hydrogen is involved in hydrogen bonded ring $R_2^1(6)$ with fluoride as acceptor (figure 2(a)).

Chains of hydrogen bonded octahedra (figure 2(b)) are linked in both *b* and *c* directions by further HBs. Within the *ac* plane, chain-like arrangement of fused $R_4^2(8)$ and $R_6^4(12)$ ring systems should be mentioned (figure 2(a)). In the *ab* plane, CuN_4O_2 octahedra are

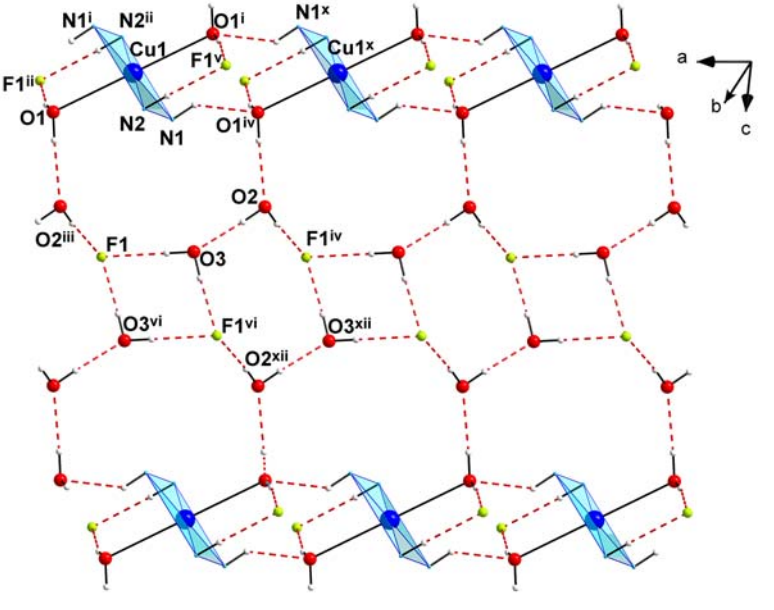

Figure 2(a). Hydrogen bonding system in **1** projected approximately into the *ac* plane. CuN_4 equatorial planes bearing the magnetic orbitals are displayed by blue color. The methyl and methylene from *bmen* are omitted for clarity. Symmetry codes: i: $2-x, -y, -z$; ii: $2-x, 1-y, -z$; iii: $1+x, y, z$; iv: $-1+x, y, z$; v: $x, -1+y, z$; vi: $1-x, 1-y, 1-z$; *x*: $1-x, -y, -z$, xii: $-x, 1-y, 1-z$.

linked by a pair of (H)O–H···F···H–O(H) HBs forming a ring system $R_6^4(12)$; these rings are linked by hydrogen bonded chains C(16). The formed hydrogen bonding system in **1** is entirely different from that observed in analogous $[Cu(en)_2(H_2O)_2]F_2{\cdot}4H_2O$ [13] in

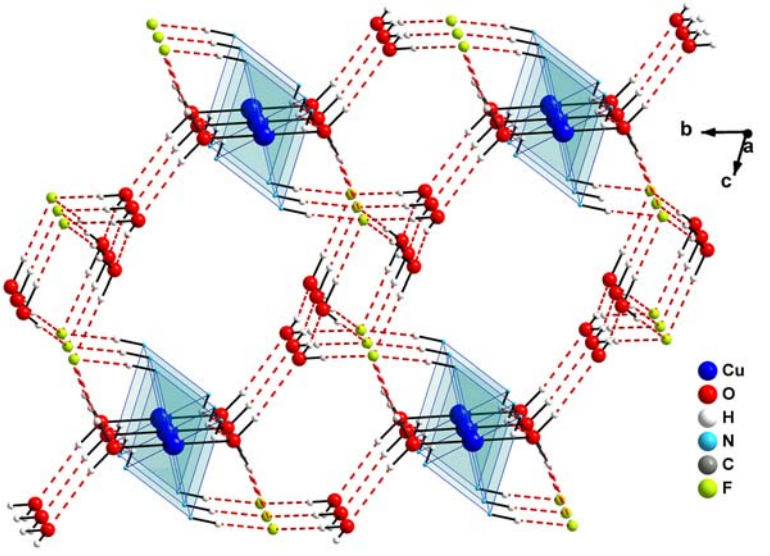

Figure 2(b). Overall view of the hydrogen bonding system in **1** along the *a* axis. CuN_4 equatorial planes bearing the magnetic orbitals are displayed by blue color. The methyl and methylene groups from *bmen* are omitted for clarity.

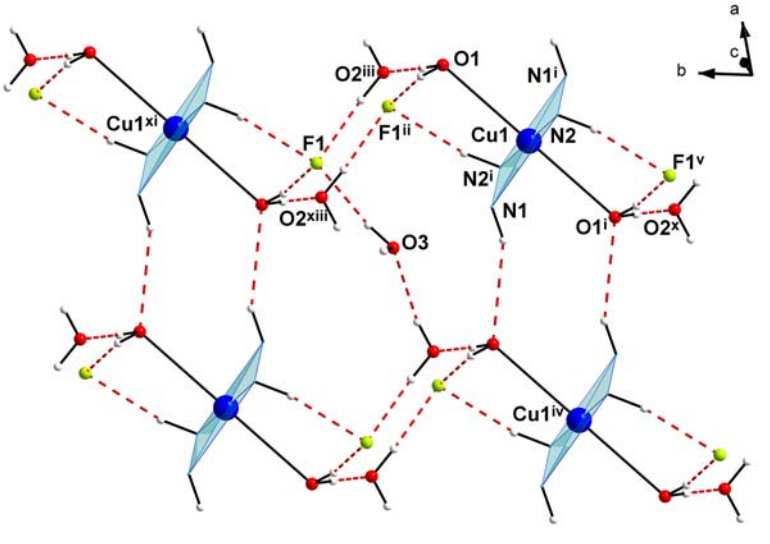

Figure 2(c). Hydrogen bonding system in **1** projected approximately into the *ab* plane. CuN_4 equatorial planes bearing the magnetic orbitals are displayed by blue color. The methyl and methylene groups from *bmen* are omitted for clarity. Symmetry codes: i: $2-x, -y, -z$; ii: $2-x, 1-y, -z$; iii: $1+x, y, z$; iv: $-1+x, y, z$; v: $x, -1+y, z$; x: $1-x, -y, -z$; xi: $x, 1+y, z$; xiii: $1-x, 1-y, -z$.

which the neighboring CuN_4O_2 octahedra are almost coplanar (the angle between neighboring equatorial planes CuN_4 is 20.26(14)°) and two different orientations of the CuN_4O_2 octahedra are present (angle between neighboring O–Cu–O lines is 86.47(4)°).

The shortest Cu···Cu distance along the *a* axis is 6.5995(5) Å for Cu1 and $Cu1^{iv}$ (iv: $-1+x, y, z$) and 8.2790(5) Å for Cu···Cu distance along the *b* axis for Cu1 and $Cu1^{xi}$ (xi: $x, 1+y, z$) (figure 2(c)). In **1,** the corresponding CuN_4 planes on the closest hydrogen bonded Cu(II) (Cu1 and $Cu1^{iv}$; iv: $-1+x, y, z$) are coplanar but the normal distance between these CuN_4 planes is 4.4378(1) Å, which suggests unfavorable arrangement of the magnetic orbitals for magnetic exchange interactions.

3.3.2. [Cu(*bmen*)$_2$(BF$_4$)$_2$)] (2). Complex **2** (figure 3) exhibits a molecular structure analogous to that reported for $[Cu(en)_2(BF_4)_2]$ [14]. Cu(II) is six-coordinate in the elongated 4 + 2 form like **1**. In the equatorial plane, two chelate *bmen* are placed with mean value of 2.035(17) Å for Cu–N bonds (table 2); this value corresponds to the mean value of 2.032 (29) Å in $[Cu(deen)_2(BF_4)_2]$ [11] and is very close, within experimental errors, to the values of 2.024(21) and 2.025(5) Å found in $[Cu(men)_2(BF_4)_2]$ [6a] and $[Cu(en)_2(BF_4)_2]$ [14], respectively. The axial positions around Cu(II) are occupied by fluorines from two tetrafluoroborates.

The tetrafluoroborate is disordered (see experimental part) and the corresponding atoms exhibit large thermal motion. Disorder associated with this anion is not uncommon, it was already observed, e.g. in $[Cu(pz)_2(BF_4)_2]$ (*pz* = pyrazine) [26] or $[Cu(ddad)(BF_4)_2]$ (*ddad* = 3,6-dimethyl-1,8-(3,5-dimethyl-1-pyrazolyl)-3,6-diaza-octane) [27]. Due to the observed disorder of BF_4^-, the axial Cu–F bond exhibits a value of 2.426(3) Å (2*x*) for the more populated position (s.o.f. = 0.685(13)) while for the less populated position (s.o.f. = 0.315(13)), the coordinating fluorine is at longer distances of 2.629(8) Å (2*x*). In similar compounds containing CuN_4F_2, the usual values for Cu–F_{ax} bonds are 2.393(31)–2.683 (16) Å; the lower value was observed in $[Cu(pyr)_4(BF_4)_2]$ (*pyr* = pyrimidine) [28] while the higher value was found in $[Cu(dpyr)_2(BF_4)_2]\cdot(CH_3)_2CO$ (*dpyr* = 3,5-dimethyl-4-iodopyrazol-1-yl)methyl) [29]; in the structure of $[Cu(en)_2(BF_4)_2]$, the corresponding value for Cu–F_{ax} bond is 2.560(1) Å (room temperature data) [14].

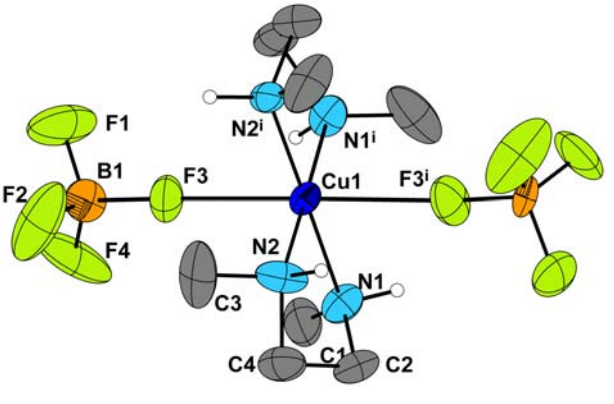

Figure 3. The molecular structure of **2**. Only the more populated positions (s.o.f. = 0.685(13)) of the fluorines are shown. The thermal ellipsoids are drawn at 30% probability level. Hydrogens from methyl and methylene from *bmen* are omitted for clarity. Symmetry code: i: $-x, y, -z$.

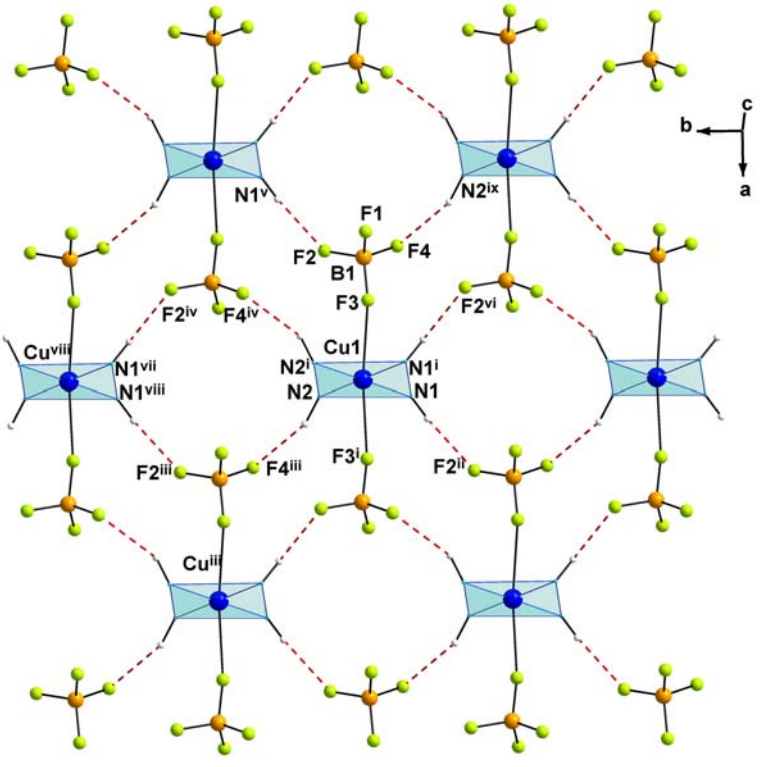

Figure 4(a). View of the hydrogen bonded layers in **2** displaying the formation of ring systems $R_4^4(16)$. Symmetry codes: i: −x, y, −z; ii: 1/2+x,−1/2 + y, z; iii: 1/2 + x, 1/2 + y, z; iv: −1/2 + x, 1/2 + y, −z; v: −1/2−x, −1/2 + y, −z; vi: −1/2−x, −1/2+ y, −z; vii: −x, 1+y, −z; viii: x, 1+y, z; ix: −1/2 + x, −1/2 + y, z.

N–H···F HBs play a crucial role in packing of the individual molecules in **2** (table 4). As can be seen in figure 4(a), for the more populated orientation of the BF_4^-, a 2D supramolecular hydrogen bonded system is formed which can be described as $R_4^4(16)$ (see also figure 4(b)). Within the hydrogen bonded layer, the shortest distance between Cu(II)s is 7.937(5) Å (Cu1···Cu1^{iii}, iii: 1/2 + *x*, 1/2 + *y*, *z*) while the second shortest distance is 8.803 (9) Å for Cu···Cu1$^{viii}_{ax}$ (viii: *x*, 1 + *y*, *z*); this distance is important for magnetic exchange interactions as the involved CuN_4 planes bearing the magnetic orbitals are coplanar. In the *b* direction, a 1D arrangement of Cu(II)s is formed. Between the hydrogen bonded layers (direction of *c* axis), only weak hydrogen bonding interactions of the C–H···F type exist (C2···F4^x 3.436(11) Å, H2A···F4^x 2.624(7) Å; C–H···F 139.3(5) Å; x: − *x*, *y*, 1 − *z*).

3.4. *Magnetic measurements*

Two possible orientations of BF_4^- in **2** lead to coexistence of two tetragonally elongated octahedral Cu(II) ions due to the different distances between Cu(II) and fluorine from the disordered BF_4^-. At 173 K, more populated (68.5%) orientation of BF_4^- yields shorter distance between Cu(II) and fluorine (2.426(3) Å) while for the less populated orientation, the Cu–F distance is 2.629(8) Å and the coordination of Cu(II) can be considered as square-

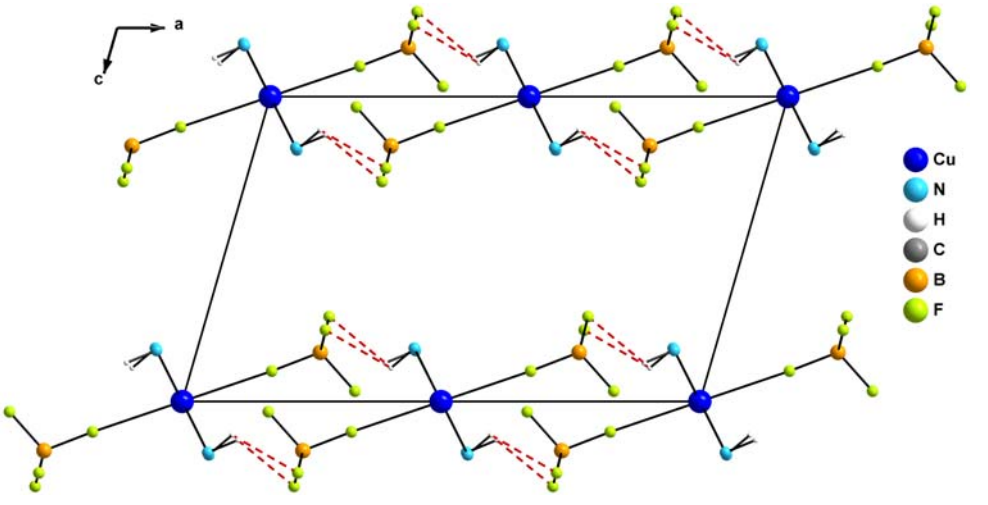

Figure 4(b). View of the hydrogen bonded layers in **2** along the *b* axis. The methyl and methylene from *bmen* are omitted for clarity. Only the more populated position of BF_4^- is shown.

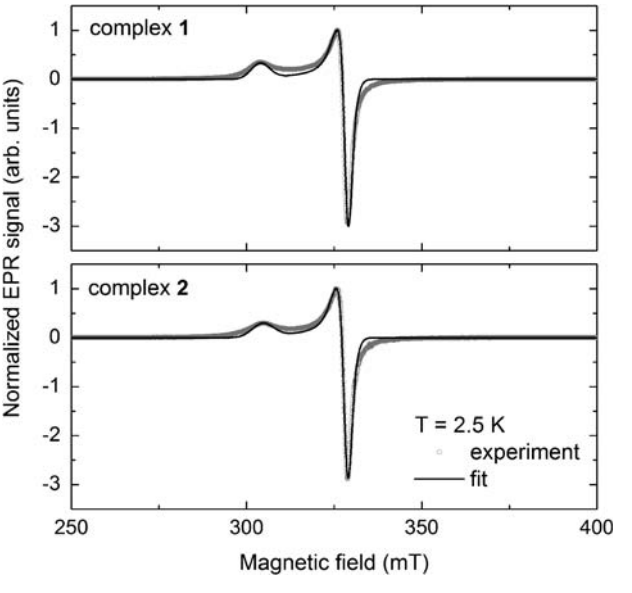

Figure 5. Comparison of the experimental EPR spectra of both complexes (circles) measured at 2.5 K (frequency is 9.4 GHz) and the EasySpin [31] fit; parameters are presented in the text.

planar, too. Although the $d_{x^2-y^2}$ electronic state, in which one unpaired electron resides, is the same for octahedral and square-planar configuration of Cu(II), the *g*-factor values depend on the energy difference between $d_{x^2-y^2}$ and d_{xy}, d_{yz}, and d_{xz} orbitals, which is larger for square-planar coordination [30]. Thus, the contribution of two slightly different *g*-tensors in **2** may be observed, but it was not resolved in the EPR spectra.

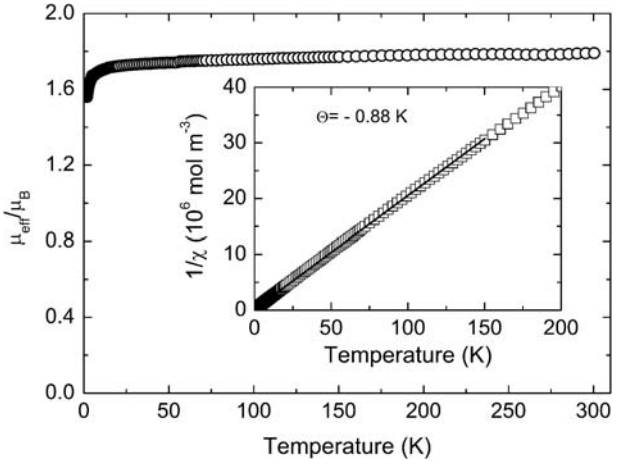

Figure 6. Temperature dependence of effective magnetic moment of **1** (circles). Inset: Curie–Weiss law fit (solid line) of the inverse susceptibility of **1** (squares).

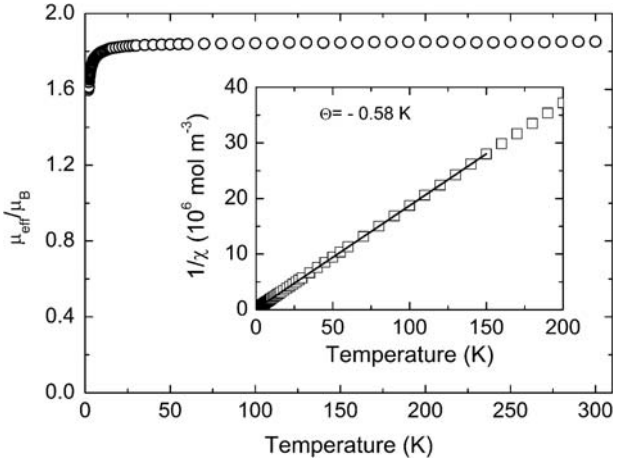

Figure 7. Temperature dependence of effective magnetic moment of **2** (circles). Inset: Curie–Weiss law fit (solid line) of the inverse susceptibility of **2** (squares).

EPR spectra of **1** and **2** at 2.5 K on powdered samples were analyzed using the EPR simulation package EasySpin (figure 5) [31]. The best agreement with experimental data was obtained for the following principal values of the *g*-tensor: $g_x = 2.044$, $g_y = 2.047$, and $g_z = 2.210$ for **1** and $g_x = 2.045$, $g_y = 2.048$, and $g_z = 2.205$ for **2**. The anisotropic *g*-factors (g_x, $g_y < g_z$) are consistent with axial anisotropy due to the Jahn–Teller effect typical for $S = 1/2$ Cu(II) and the exchange paths will propagate along the directions determined by lobes of the $d_{x^2-y^2}$ orbital in the planes of *bmen*. The hyperfine structure expected for Cu (II) could not be resolved in the spectrum, suggesting the existence of exchange couplings between magnetic centers [32]. An anisotropic broadening of the resonance line (full width at half height) $\Delta B = [\Delta B_x, \Delta B_y, \Delta B_z] = [2.14, 5.35, 6.78]$ mT for **1** and $\Delta B = [\Delta B_x, \Delta B_y,$

$\Delta B_z] = [2.32, 5.35, 7.85]$ mT for **2** described the resonance line. An anisotropic linewidth broadening can reflect the unresolved hyperfine structure and the low-dimensional character of the magnetic subsystem in both complexes.

For estimation of the exchange coupling of both complexes, we measured the temperature dependence of the magnetic susceptibility of polycrystalline samples. The effective magnetic moment extracted from the magnetic susceptibility at 300 K is $\mu_{eff} = 1.79\,\mu_B$ and $\mu_{eff} = 1.85\,\mu_B$ in **1** and **2**, respectively. The susceptibility of both complexes shows a Curie–Weiss-like behavior (reflected in the linear temperature dependence of the inverse susceptibility in the inset of figures 6 and 7) but the sharp decreases of the effective magnetic moments below 10 K suggest the presence of antiferromagnetic exchange coupling. A Curie–Weiss fit to the inverse susceptibility from 1.8 to 150 K yielded the Curie temperature $\theta = -0.88$ K and $g = 2.04$ for **1** (inset of figure 6) and $\theta = -0.58$ K and $g = 2.13$ for **2** (inset of figure 7), suggesting the presence of weak antiferromagnetic coupling in both complexes. Such weak coupling is not unusual taking into account the large distance between Cu(II) ions and unfavorable mutual orientation of $d_{x^2-y^2}$ orbitals between $[Cu(bmen)_2(H_2O)_2]^{2+}$ in **1** and $[Cu(en)_2(BF_4)_2]$ in **2** as obtained from the structural and EPR analyses. We suggest that the exchange coupling is propagated through the network of HBs as observed in several complexes with tetracyanidometallate anions [7–9] and fluorine-based anions [6a, 10].

4. Conclusions

Two Cu(II) complexes with anions based on fluorine, $[Cu(bmen)_2(H_2O)_2]F_2{\cdot}4H_2O$ (**1**), and $[Cu(bmen)_2(BF_4)_2]$ (**2**), were prepared and characterized. While **1** exhibits ionic crystal structure, **2** is built up of complex molecules; in both crystal structures, extended networks of HBs are present. In both **1** and **2,** Cu(II) is six-coordinate in the 4 + 2 form with *trans*-CuN_4O_2 and *trans*-CuN_4F_2 chromophores, respectively. Magnetic studies from 1.8 to 300 K reveal that **1** and **2** follow the Curie–Weiss law with parameters $\theta = -0.88$ K and $g = 2.04$ for **1** and $\theta = -0.58$ K and $g = 2.13$ for **2**; the observed values suggest the presence of weak antiferromagnetic interactions between Cu(II) ions mediated by HBs in both complexes in line with literature data on similar Cu(II) complexes [9, 33, 34].

Supplementary materials

Crystallographic data for **1** (CCDC 86690) and **2** (CCDC 866901) has been deposited with the Cambridge Crystallographic Data Center. Copies of the information may be obtained free of charge from The Director, CCDC, 12 Union Road, Cambridge, CB21EZ, UK (Fax:+44 1223 336033; E-mail: deposit@ccdc.cam.ac.uk or www: http://www.ccdc.cam.ac.uk).

Acknowledgements

This work was supported by the Slovak grant agency VEGA (Grant Nos. 1/0089/09 and 1/0078/09), Slovak Research and Development Agency (Grant No. APVV-0132-11), SAS Center of Excellence: CFNT MVEP and ERDF EU (European Union European regional development fond) grant, under the contract No. ITMS26220120047. J.H. thanks the

support from P.J. Šafárik, University in Košice, Faculty of Sciences Student grant (VVGS 1/12-13). Material support from US Steel – DZ Energetika Košice is greatly acknowledged. We thank M. Kajňaková for SQUID data collection.

References

[1] G.A. Jeffrey. *An Introduction to Hydrogen Bonding*, Oxford University Press, Oxford (1997).
[2] G. Gilli, P. Gilli. *The Nature of the Hydrogen Bond*, Oxford University Press, Oxford (2009).
[3] J.S. Costa, N.A.G. Bandeira, B.L. Guennic, V. Robert, P. Gamez, G. Chastanet, L. Ortiz-Frade, L. Gasque. *Inorg. Chem.*, **50**, 5696 (2011).
[4] P. Baran, R. Boča, M. Breza, H. Elias, H. Fuess, V. Jorík, R. Klement, I. Svoboda. *Polyhedron*, **21**, 1561 (2002).
[5] C. Desplanches, E. Ruiz, A. Rodriguez-Fortea, S. Alvarez. *J. Am. Chem. Soc.*, **124**, 5197 (2002).
[6] (a) J. Černák, J. Haníková, J. Kuchár, E. Čižmár, Z. Trávniček. *J. Mol. Struct.*, **963**, 71 (2010); (b) J. Černák, M. Orendáč, I. Potočňák, J. Chomič, A. Orendáčová, J. Skoršepa, A. Feher. *Coord. Chem. Rev.*, **224**, 51 (2002).
[7] J. Hanko, M. Orendáč, J. Kuchár, Z. Žák, J. Černák, A. Orendáčová, A. Feher. *Solid State Commun.*, **142**, 128 (2007).
[8] I. Potočnák, M. Vavra, E. Čižmár, M. Kajňáková, A. Radváková, D. Steinborn, S.A. Zvyagin, J. Wosnitza, A. Feher. *J. Solid State Chem.*, **182**, 196 (2009).
[9] J. Kuchár, J. Černák, Z. Mayerová, P. Kubáček, Z. Žák. *Solid State Phenom.*, **90–91**, 323 (2003).
[10] J. Haníková, J. Černák, J. Kuchár, E. Čižmár. *Inorg. Chim. Acta*, **385**, 178 (2012).
[11] B. Narayanan, M.M. Bhadbhade. *J. Coord. Chem.*, **46**, 115 (1998).
[12] C.C. Su, C.Y. Wu. *J. Coord. Chem.*, **33**, 1 (1994).
[13] J. Emsley, M. Arif. *J. Mol. Struct.*, **220**, 1 (1990).
[14] D.S. Brown. *Acta Cryst.*, **B24**, 730 (1968).
[15] O. Kahn. *Molecular Magnetism*, Wiley, New York, NY (1985).
[16] Oxford Diffraction. *CrysAlis RED and CrysAlis CCD software (Version 1.171.1)*, Oxford Diffraction Ltd., Abingdon, England (2003).
[17] G.M. Sheldrick. *Acta Cryst.*, **A64**, 112 (2008).
[18] L.J. Farrugia. *J. Appl. Cryst.*, **32**, 837 (1999).
[19] M. Nardelli. *J. Appl. Cryst.*, **32**, 563 (1999).
[20] K. Brandenburg. *DIAMOND, Crystal Impact (Version 3.1f) GbR*, Bonn, Germany (2008).
[21] K. Nakamoto. *Infrared and Raman Spectra of Inorganic and Coordination Compounds,* Part B: Applications in Coordination, Organometallic, and Bioinorganic Chemistry, Wiley, New York, NY (1997).
[22] I.M. Procter, B.J. Hathaway, P. Nicholls. *J. Chem. Soc.*, (1968).
[23] H. Icbudak, H. Olmez, O.Z. Yesilel, F. Arslan, P. Naumov, G. Jovanovski, A.R. Ibrahim, A. Usman, H.-K. Fun, S. Chantrapromma, S.W. Ng. *J. Mol. Struct.*, **657**, 255 (2003).
[24] J. Bernstein, R.E. Davis, L. Shimoni, N.-L. Chang. *Angew. Chem. Int. Ed.*, **34**, 1555 (1995).
[25] M.C. Etter, J. MacDonald, J. Bernstein. *Acta Cryst.*, **B46**, 256 (1990).
[26] F.M. Woodward, P.J. Gibson, G. Jameson, C.P. Landee, M.M. Turnbull, R.D. Willett. *Inorg. Chem.*, **46**, 4256 (2007).
[27] W.G. Haanstra, W.L. Driessen, R.A.G. de Graaff, G.C. Sebregts, J. Suriano, J. Reedijk, U. Turpeinen, J.S. Wood. *Inorg. Chim. Acta*, **189**, 243 (1991).
[28] B. Novak, S.W. Keller. *J. Chem. Cryst.*, **27**, 279 (1997).
[29] E.V. Lider, E.V. Peresypkina, L.G. Lavrenova, O.L. Krivenko, E.G. Boguslavsky, A.I. Smolentsev, L.A. Sheludyakova, S.F. Vasilevsky. Koord. Khim. (Russ.). *Coord. Chem.*, **35**, 442 (2009).
[30] B.J. Hathaway, D.E. Billing. *Coord. Chem. Rev.*, **5**, 143 (1970).
[31] S. Stoll, A. Schweiger. *J. Magn. Reson.*, **178**, 42 (2006).
[32] A. Bencini, D. Gatteschi. *Electron Paramagnetic Resonance of Exchange Coupled Systems*, Springer, Berlin (1990).
[33] H. Li, S.G. Zhang, L.M. Xie, L. Yu, J.M. Shi. *J. Coord. Chem.*, **64**, 1456 (2011).
[34] S.R. Choudhury, C.Y. Chen, S. Seth, T. Kar, H.M. Lee, E. Colacio, S. Mukhopadhyay. *J. Coord. Chem.*, **62**, 540 (2009).